Impact of Front Range sources on reactive nitrogen concentrations and deposition in Rocky Mountain National Park

Katherine B. Benedict [Corresp., 1] , Anthony J Prenni [2] , Amy P Sullivan [1] , Ashley R Evanoski-Cole [1, 3] , Emily V Fischer [1] , Sara Callahan [1] , Barkley C Sive [2] , Yong Zhou [1] , Bret A Schichtel [4] , Jeffrey L Collett Jr. [1]

[1] Department of Atmospheric Science, Colorado State University, Fort Collins, Colorado, United States

[2] Air Resources Division, National Park Service, Lakewood, CO, US

[3] now at Department of Chemistry, St. Bonaventure University, St. Bonaventure, NY, United States

[4] Air Resources Division, National Park Service, Fort Collins, CO, US

Corresponding Author: Katherine B. Benedict
Email address: katherine.benedict@colostate.edu

Human influenced atmospheric reactive nitrogen (RN) is impacting ecosystems in Rocky Mountain National Park (ROMO). Due to ROMO's protected status as a Class 1 area, these changes are concerning and improving our understanding of the contributions of different types of RN and their sources is important for reducing impacts in ROMO. In July-August 2014 the most comprehensive measurements (to date) of RN were made in ROMO during the Front Range Air Pollution and Photochemistry Éxperiment (FRAPPÉ). Measurements included peroxyacetyl nitrate (PAN), C_1-C_5 alkyl nitrates, and high-time resolution NO_x, NO_y, and ammonia. A limited set of measurements was extended through October. Co-located measurements of a suite of volatile organic compounds provide information on source types impacting ROMO. Specifically, we use ethane as a tracer of oil and gas operations and tetrachloroethylene (C_2Cl_4) as an urban tracer to investigate their relationship with RN species and transport patterns. Results of this analysis suggest elevated RN concentrations are associated with emissions from oil and gas operations, which are frequently co-located with agricultural production and livestock feeding areas in the region, and from urban areas. There also are periods where reactive nitrogen at ROMO is impacted by long-range transport. We present an atmospheric RN budget and a nitrogen deposition budget with dry and wet components. Total deposition for the period (7/1-9/30) was estimated at 1.58 kg N/ha, with 87% from wet deposition during this period of above average precipitation. Ammonium wet deposition was the dominant contributor to total nitrogen deposition followed by nitrate wet deposition and total dry deposition. Ammonia was estimated to be the largest contributor to dry deposition followed by nitric acid and PAN (other species included alkyl nitrates, ammonium and nitrate). All three species are challenging to measure routinely, especially at high time resolution.

Impact of Front Range Sources on Reactive Nitrogen Concentrations and Deposition in Rocky Mountain National Park

11 Katherine B. Benedict[1], Anthony J. Prenni[2], Amy P. Sullivan[1], Ashley R Evanoski-Cole[1,3],
12 Emily V. Fischer[1], Sara Callahan[1], Barkley C. Sive[2], Yong Zhou[1], Bret A Schichtel[4], Jeffrey L.
13 Collett, Jr. [1]

15 [1]Department of Atmospheric Science, Colorado State University, Fort Collins, CO, USA

16 [2]National Park Service, Air Resources Division, Lakewood, CO, USA

17 [3]now at Department of Chemistry, St. Bonaventure University, St. Bonaventure, NY, USA

18 [4]National Park Service, Air Resources Division, Fort Collins, CO, USA

23 **Abstract**

24 Human influenced atmospheric reactive nitrogen (RN) is impacting ecosystems in Rocky

25 Mountain National Park (ROMO). Due to ROMO's protected status as a Class 1 area, these

26 changes are concerning and improving our understanding of the contributions of different types

27 of RN and their sources is important for reducing impacts in ROMO. In July-August 2014 the

28 most comprehensive measurements (to date) of RN were made in ROMO during the Front Range

29 Air Pollution and Photochemistry Éxperiment (FRAPPÉ). Measurements included peroxyacetyl

30 nitrate (PAN), C_1-C_5 alkyl nitrates, and high-time resolution NO_x, NO_y, and ammonia. A limited

31 set of measurements was extended through October. Co-located measurements of a suite of

32 volatile organic compounds provide information on source types impacting ROMO.

33 Specifically, we use ethane as a tracer of oil and gas operations and tetrachloroethylene (C_2Cl_4)

34 as an urban tracer to investigate their relationship with RN species and transport patterns.

35 Results of this analysis suggest elevated RN concentrations are associated with emissions from

36 oil and gas operations, which are frequently co-located with agricultural production and livestock

37 feeding areas in the region, and from urban areas. There also are periods where reactive nitrogen

38 at ROMO is impacted by long-range transport. We present an atmospheric RN budget and a

39 nitrogen deposition budget with dry and wet components. Total deposition for the period (7/1-

40 9/30) was estimated at 1.58 kg N/ha, with 87% from wet deposition during this period of above

41 average precipitation. Ammonium wet deposition was the dominant contributor to total nitrogen

42 deposition followed by nitrate wet deposition and total dry deposition. Ammonia was estimated

43 to be the largest contributor to dry deposition followed by nitric acid and PAN (other species

44 included alkyl nitrates, ammonium and nitrate). All three species are challenging to measure

45 routinely, especially at high time resolution.

1.0 Introduction

The nitrogen cycle has been altered by increasing production of reactive nitrogen (RN) for food production and energy (Galloway et al., 2008). Much of the reactive nitrogen produced ultimately ends up in air and water, potentially contributing to environmental problems (Fenn et al., 1998; Howarth, 2004). Direct leaching from fertilized soils contributes to eutrophication of fresh water. Emissions to the atmosphere can increase ozone and particle formation as well as contribute to elevated nitrogen deposition to land surfaces and water bodies. Elevated nitrogen deposition can alter ecosystems and the services they provide in many regions (Goulding et al., 1998; Fenn et al., 2003; Burns, 2004; Bell et al., 2017) as many ecosystems are nitrogen limited (LeBauer & Treseder, 2008). Across the globe there has been intense focus on understanding levels of nitrogen deposition and its impacts in particularly sensitive and protected ecosystems. Over the past several decades, researchers in Europe, the United States, and China have focused on better understanding the interactions and changes in ecosystems that occur as a result of excess reactive nitrogen deposition using long-term networks. An extensive network was established throughout Europe in 2006-2011 to measure ambient RN concentrations, estimate dry deposition and provide a comprehensive data set for regional models (Owen et al., 2011; Flechard et al., 2011). In contrast, work in the United States has focused primarily on wet nitrogen deposition measurements made by the National Atmospheric Deposition Program (NADP) (Lehmann, Bowersox & Larson, 2005). In China there has not been a long-term national deposition monitoring program; however there has been an effort to implement long-term standardized nitrogen deposition measurements (Liu et al., 2011).

In the United States, one area of focus has been aimed at Rocky Mountain National Park (ROMO), a high elevation site which includes alpine tundra and lakes, exposed bedrock, and

70   subalpine forests (Baron et al., 1994). The Rocky Mountains are more susceptible to reactive

71   nitrogen deposition than many other areas because nitrogen is not well retained in the local soil

72   and plants. Reduced plant nitrogen demand results from a short growing season, which

73   decreases nitrogen retention. Additionally, the soil types in the area (exposed bedrock, talus,

74   coarse soils) reduce contact time between drainage water and soil (Fenn et al., 1998).

75   Research aimed at improved understanding of nitrogen deposition in ROMO has been

76   ongoing for many years (Bowman & Steltzer, 1998; Burns, 2003, 2004; Baron et al., 2004;

77   Baron, 2006; Beem et al., 2010; Benedict et al., 2013c,a). Several studies have demonstrated

78   that increased nitrogen deposition has been associated with changes in biological species and

79   ecological processes (Bowman & Steltzer, 1998; Burns, 2004; Baron, 2006), and a high spatial

80   variability of nitrogen deposition in the region has been observed from national monitoring

81   network data (Burns, 2003; Beem et al., 2010). Measurements characterizing many reactive

82   nitrogen species are routinely collected in the park as part of NADP, the Interagency Monitoring

83   of Protected Visual Environments (IMPROVE) program, the Clean Air Status and Trends

84   Network (CASTNET), and the Ammonia Monitoring Network (AMoN). These networks

85   provide the data needed for tracking progress toward reduction of nitrogen deposition in ROMO,

86   a goal mutually set by the State of Colorado, the US EPA, and the National Park Service

87   (CDPHE, 2017). Special studies like the Rocky Mountain Atmospheric Nitrogen and Sulfur

88   (RoMANS) Studies (Malm et al., 2009) have increased the understanding of the type and

89   frequency of atmospheric transport that plays a role in atmospheric nitrogen inputs into the

90   ecosystems at ROMO as well as the importance of wet organic nitrogen deposition and dry

91   deposition of ammonia (NH_3) (Beem et al., 2010; Benedict et al., 2013c,a).

92   The Front Range Air Pollution and Photochemistry Experiment (FRAPPÉ) was

93   conducted July 15 through August 18, 2014. Although the primary goal of FRAPPÉ was to

94   better characterize summertime air quality in the Northern Front Range Metropolitan Area

95   (NFRMA), the extensive suite of measurements collected during FRAPPÉ allowed for

96   determination of the degree to which pollution from NFRMA sources and long-range transport

97   contribute to air quality impacts at ROMO. FRAPPÉ was conducted in parallel with the 2014

98   DISCOVER-AQ (Deriving Information on Surface Conditions from Column and Vertically

99   Resolved Observations Relevant to Air Quality) project in Colorado. Research flights, surface

100   mobile measurements, and stationary ground sites were coordinated to provide a comprehensive

101   picture of the atmospheric processes impacting air quality in the northern Front Range. The

102   majority of operations took place along the Front Range, near the main pollutant sources in the

103   region, although research flights and several ground sites characterized more remote areas to

104   better understand the transport and impact from the source regions.

105   In this manuscript, we describe measurements made during FRAPPÉ from a ground site

106   collocated with routine monitoring measurements at the Rocky Mountain National Park Longs

107   Peak (ROMO-LP) field site. Measurements began July 7, prior to the FRAPPÉ study period, and

108   continued through October 15, well after the campaign ended. These measurements included

109   high time resolution (1 min to 1 hour) NH_3, nitric oxide (NO), and NO_y ($\sum$oxidized nitrogen)

110   concentrations, as well as more comprehensive 24-hour gas (NH_3, nitric acid - HNO_3, sulfur

111   dioxide - SO_2) and particle chemistry (ammonium-NH_4^+, nitrate-NO_3^-, sulfate - SO_4^{2-}, sodium -

112   Na^+, potassium - K^+, magnesium - Mg^{2+}, calcium - Ca^{2+}, and chloride - Cl^-) measurements.

113   Two gas chromatographs were used to measure select organic nitrogen species including

114   peroxyacetyl nitrate (PAN), methyl nitrate ($MeONO_2$), ethyl nitrate ($EtONO_2$), i-propyl nitrate

115 (iPrONO$_2$), 2-butyl nitrate (2BuONO$_2$), 2-pentyl nitrate (2PenONO$_2$), and 3-pentyl nitrate

116 (3PenONO$_2$); as well as volatile organic compound (VOC) tracers for a variety of sources.

117 These measurements were aimed at better understanding the sources that contribute to pollutant

118 concentrations in ROMO, specifically for RN species. We provide a comprehensive budget for

119 RN in ROMO during FRAPPÉ, calculate a nitrogen deposition budget, and assess important

120 sources for the primary components of the RN budget.

121

122 **2.0 Methods**

123 The measurement site at ROMO (Figure 1) was located south of Estes Park, CO, near the base of

124 Longs Peak. The site (40.2783°, -105.5457°; 2784 m ASL) is co-located with IMPROVE

125 (ROMO1) and CASTNet (ROM206/406) national network monitoring sites, and the National

126 Park Service Gaseous Pollutant Monitoring Network (GPMP). Measurements were conducted

127 both in the GPMP shelter and in the National Park Service/Colorado State University Mobile Air

128 Quality Laboratory stationed at the site.

129
130
131 *2.1 High-time resolution NH$_3$ and NO$_y$*

132   High-time resolution (~ 5 sec) measurements of NH$_3$ were made using a Picarro G1103

133 Analyzer, a cavity ring-down spectroscopy instrument, located in mobile laboratory. The inlet

134 line (Teflon tubing) was located approximately 6 m above ground level (agl). The entire length

135 of the inlet line was insulated and heated to 40°C to minimize wall losses. A filter (Picarro P/N

136 S1021) was placed on the end of the inlet to prevent particles from entering the instrument.

137 Ammonium nitrate captured by the filter likely volatilized on the heated filter during sampling

138 and is a potential source of bias in the NH$_3$ measurement. However, concurrent 24-hr averaged

139   measurements from an annular denuder/filter-pack sampler (see below) suggest that, assuming

140   that all of the NH_4NO_3 sublimates and is measured as NH_3, the median bias in the measurements

141   was 7.7%. A correction was not applied to the final dataset. Calibrations were performed at the

142   beginning and end of the field deployment with a known concentration of ammonia, generated

143   using a calibration gas diluted with a Teledyne Zero Air Generator (Model 701). A phosphorus

144   acid (10% w/v) coated denuder operated in parallel confirmed the supplied NH_3 concentration.

145   The mobile lab, which housed the instrument, had an air conditioning failure July 23-30 resulting

146   in conditions that were too hot for proper operation of the Picarro. After A/C was restored, a

147   section of the heated inlet overheated and this problem was not discovered until August 8. Thus

148   NH_3 data for the period July 23 – August 9 are omitted from this analysis.

149   CASTNET NO_y and NO data were downloaded from www.epa.gov/castnet (U.S.

150   Environmental Protection Agency Clean Air Markets Division, 2016a). A Teledyne API

151   T200U/NO_y instrument is operated at the ROMO CASTNET site (ROM206). This instrument

152   measures both NO_y and NO by chemiluminescence. NO is directly measured and NO_y is

153   converted using a thermal catalytic converter and measured as NO (US EPA, 2017). This method

154   has an uncertainty of $\leq\pm10\%$ with the additional caveats that some reduced organic nitrogen

155   compounds may be converted and the conversion of the different NO_y species is highly

156   temperature dependent (Crosley, 1996; Kondo et al., 1997; Williams et al., 1998). The site is

157   operated in accordance with the Quality Assurance Plan for Procuring, Installing, and Operating

158   NCore Air Monitoring Equipment at CASTNET sites (Amec Foster Wheeler, 2016).

159

160   *2.2 High-time resolution organic compounds*

161   An *in situ* gas chromatography (GC) system was setup in the mobile laboratory located at

162   the ROMO site to measure hourly concentrations of select VOCs. This is a cryogen-free

163   concentration and analysis system consisting of two GCs coupled to 4 columns. A VF-1701

164   (Varian Inc.) was used with an electron capture detector (ECD) for C1-C2 halocarbons and C1-

165   C5 alkylnitrates; a Flame Ionization Detector (FID) was used with the three other columns: CP-

166   Al_2O_3/Na_2SO_4 PLOT for detection of C_2-C_7 hydrocarbons, VF-1ms for C_6-C_{10} hydrocarbons and

167   a PoraBond Q column for selected oxygenated VOCs (OVOCs). The system, calibrated daily, is

168   similar to those used in other studies (Sive et al., 2005; Abeleira et al., 2017). The GC was

169   located in the mobile lab, data are unavailable for the July 23-30 period of the A/C failure.

170   Peroxyacetyl nitrate (PAN) was measured at ROMO using a custom gas chromatograph

171   with 15-min time-resolution in the GPMP shelter. For the ROMO 2014 deployment, this custom

172   system was configured to measure PAN, but not its homologues. The instrument operation and

173   calibration are described in Zaragoza et al (2017). Briefly, the system used a ThermQuest ECD

174   held at 50°C and calibrations were performed regularly throughout the campaign using a

175   photolysis cell to generate PAN with accurately measured flows of acetone in ultra high purity

176   zero air and NO in nitrogen (Scott-Marrin Cylinder Numbers: CB09819 and CB11156).

177

178   *2.3 24-hour inorganic gases and particles*

179   24-hour inorganic gas and $PM_{2.5}$ particle chemistry was measured using URG annular

180   denuders and filter-packs (URG Corporation, Chapel Hill, NC), replaced daily at 9:00 MDT,

181   with a nominal volumetric flow of 10 L/min. These samplers were located outside the mobile

182   laboratory at the ROMO site. Details on sample extraction and analysis can be found in previous

183   work (Beem et al., 2010; Benedict et al., 2013b,c). The collected samples were analyzed to

184 determine the concentrations of gas phase NH_3 and HNO_3 and particle phase NH_4^+, NO_3^-, SO_4^{2-},

185 K^+, Na^+, Cl^-, Mg^{2+}, and Ca^{2+}.

186

187 *2.4 Wet Deposition*

188   Precipitation samples were collected using an automated NCON Systems (Arnoldsville,

189 GA, USA) ADS/NTN Atmospheric Precipitation Sampler. Sample buckets were changed every

190 2 to 3 days depending on the site visit schedule. Sample buckets were cleaned with deionized

191 water, shaken to remove water, covered with Al foil, and allowed to dry. Blanks were taken by

192 pipetting 30 mL of high-purity deionized water into the bucket. Each bucket was weighed prior

193 to installation in the field and upon returning to the lab to determine the total sample volume

194 collected. Sample pH was measured after returning to the lab using a combination pH electrode

195 and the remaining sample was frozen until analysis. Samples were analyzed for ionic

196 composition (NH_4^+, NO_3^-, SO_4^{2-}, Na^+, K^+, Mg^{2+}, Ca^{2+}, and Cl^-) using ion chromatography

197 (Dionex) with conductivity detection and for total nitrogen by high temperature catalyzed

198 combustion with chemiluminescent analysis of NO using a Shimadzu TOC V_{CSH}+TNM-1 total

199 organic carbon analyzer with total nitrogen module (Benedict et al., 2013a).

200

201 **3.0 Results and Discussion**

202 **3.1 Overview of sampling period**

203   A timeline of the FRAPPÉ period is shown in Figure 2 for the nitrogen species

204 measured at high-time resolution, key tracer species, wind direction and precipitation. From the

205 wind direction data, we can see that consecutive days of upslope flow (shaded region, 90-180°)

206 from the Front Range, when winds are from the southeast, mainly occurred at the end of July and

207   beginning of August and then again mid-month in August. We note that because the site is

208   located in a valley, winds are channeled primarily in two directions (Figure 3): from the

209   southeast (upslope flow from the Colorado Front Range and northeast Colorado) and from the

210   northwest (from less developed areas west of the Continental Divide). From previous work we

211   know transport from the Front Range is an important source of nitrogen to ROMO (Beem et al.,

212   2010; Benedict et al., 2013c); during periods of upslope flow in 2014 we also observe increases

213   in the Front Range tracers and reactive nitrogen species. The pollution rose for PAN is shown as

214   an example (Figure 3) of the higher concentrations of reactive nitrogen species associated with

215   upslope flow. This pattern of higher concentrations being associated with southeast (upslope)

216   flow is similar for all of the reactive nitrogen species measured. On August 11 and 12 there were

217   strong upslope winds and NH_3 was the highest observed during the FRAPPE study period.

218   Others have suggested a fire influence in the Front Range during the August 11 and 12 period

219   (Dingle et al., 2016), which may also contribute to reactive nitrogen concentrations (Benedict et

220   al., 2017).   Other upslope periods (e.g., July 22) show stronger signals in tracer species

221   compared to NH_3. Throughout the study period, there appear to be strong correlations between

222   the peak concentrations of PAN, $R-ONO_2$, ethane, and C_2Cl_4, suggesting similar sources and/or

223   source regions, and NO_y concentration timelines share similarities to PAN. Unfortunately, due

224   to air conditioner failures, limited data were collected for portions of the study period.

225   To improve our understanding of the sources and relationships between compounds, we

226   next examine the diurnal cycles of several key N species (Figure 4). Most of the species have a

227   peak later in the day, likely associated with radiatively driven upslope transport, while there is an

228   early peak in ammonia which is more likely to be associated with bi-directional exchange and

229   the role of dew (Wentworth et al., 2016). An early morning peak in ammonia has been observed

230   at other sites, including in Grand Teton National Park (Prenni et al., 2014), suggesting this may

231   be a common occurrence. The early morning high concentrations of ammonia reflect local

232   environmental effects (volatilization from evaporating dew) that strongly alter morning ammonia

233   concentrations. There is no clear early morning peak of NH_3 observed in the August diurnal

234   averages shown in Figure 4, perhaps due to drier conditions. Earlier in the study (July) there

235   were several large early morning peaks that are likely related to dew evaporation. To eliminate

236   this factor from our source analysis, the morning (6 AM – 10 AM) ammonia data were removed

237   from the remainder of the analyses as any local factors that cause high NH_3 concentration would

238   confound any interpretation of correlations with other species. NO_y peaks early, between 6AM

239   and 9AM, likely related to local morning traffic and then peaks again mid-afternoon through the

240   evening with a lot of variability in when the highest late-day concentration is observed. The

241   alkyl nitrates have the latest peak in concentration and are most similar to the diurnal cycles of

242   the two tracer species (C_2Cl_4 and ethane). Concentrations of total R-ONO$_2$ are consistently low

243   from the early morning (2 AM) through noon with the highest concentrations observed between

244   5 PM and 11 PM.   On average the increases in PAN begin around 7 AM, likely associated with

245   sunrise and the initiation of photochemical reactions. PAN slowly increases throughout the day

246   with its average peak concentration occurring around 6 PM before concentrations begin to

247   decrease overnight.

248

249   *3.2 Atmospheric Reactive Nitrogen Budget*

250   The 2014 period of intensive measurements provided an opportunity to examine the

251   contribution of individual nitrogen compounds to the total atmospheric reactive nitrogen budget.

252   For the FRAPPÉ period (July 16 – August 18), NO_y species were the most abundant,

253   contributing 67% to the total RN budget (Figure 5).

254   Based on our speciated measurements, NO_y was partitioned as follows: 24% as PAN, 7%

255   as NO, 4% as alkyl nitrates, and 11% as HNO_3 and NO_3^-. We estimate that the remaining 54%

256   was NO_2 and other unmeasured oxidized nitrogen species (NO_z). We note that we cannot

257   separate NO_2 concentrations from other NO_z contributions using the chemiluminescence

258   instrument and converter system employed during FRAPPÉ. Other potential contributors to the

259   NO_z fraction include other organo-nitrogen compounds like hydroxynitrates, isoprene nitrates,

260   and peroxyacyl nitrates other than PAN, but their importance is uncertain and is likely to vary

261   spatially and temporally (Parrish et al., 1993; Thornberry et al., 2001; Day et al., 2003). At night

262     $NO_3^\bullet$ and N_2O_5 could be important contributors to NO_y but in the presence of isoprene and

263   unsaturated alkenes are likely to react, photolyze to NO_2 at sunrise, or, in the case of N_2O_5,

264   undergo hydrolysis on aerosols to form particulate NO_3^- (Brown S. S. et al., 2004; Brown et al.,

265   2006). Previous measurements in Boulder and Denver show large temporal variability with

266   concentration ranging from below detection to 100 pptv for $NO_3^\bullet$ and below detection to 3 ppbv

267   for N_2O_5 (Brown & Stutz, 2012). While the specific contribution to nitrogen deposition is

268   unknown for these species, they are expected to be captured in the NO_y measurement.

269   A subset of the RN species have been measured at ROMO in previous years. Summary

270   data from these measurements are given in Table 1. The overall partitioning between reduced

271   and oxidized reactive nitrogen (i.e. leftmost column of Figure 5) is consistent with measurements

272   from other years (2009, 2010, 2015, 2016), when only NH_3, NH_4^+, HNO_3, NO_3^-, and NO_y were

273   measured. The four other study years measured NO_y, NH_3 and NH_4^+ from July through October.

274   In this 2014 FRAPPÉ study the total RN was 1.6 ppb compared to 1.9 – 2.6 ppb in the other four

275   studies.

276   Alkyl nitrates were measured for the first time in ROMO during the 2014 FRAPPÉ study.

277   The alkyl nitrates measured here are primarily formed by oxidation of hydrocarbons emitted

278   from fossil fuels (ethane, butane, pentane) and generally contribute less than 10% to NO_y in

279   continental regions (Russo et al., 2010a). Measurements of alkyl nitrates during FRAPPÉ were

280   consistent with this, contributing 4% to NO_y and 2.7 % to the total atmospheric RN budget

281   during FRAPPÉ (Figure 5). The measured alkyl nitrates were primarily composed of i-propyl

282   nitrate (26%), methyl nitrate (25%), and 2-butyl nitrate (23%). The remaining 26% were ethyl

283   nitrate (9%), n-propyl nitrate (6%), 2-pentyl nitrate (5%), and 3-pentyl nitrate (6%). All of the

284   alkyl nitrate concentrations were highly correlated with each other, except methyl nitrate (Figure

285   6). Whereas all of the other alkyl nitrates measured are primarily photochemical oxidation

286   products, methyl nitrate ($MeONO_2$) has both a photochemical and marine source. To examine

287   the influence of a potential marine influence, we examined the relationship between ethyl nitrate

288   ($EtONO_2$) and $MeONO_2$ colored by $CHBr_3$ (Figure 6b), a tracer for marine air (Gschwend,

289   MacFarlane & Newman, 1985; Carpenter et al., 2005). As seen in the figure, $MeONO_2$ is

290   enhanced during periods with elevated $CHBr_3$, suggesting that, although ROMO is relatively

291   distant from marine sources, the park can be measurably influenced by marine air. Previous

292   results from HYSPLIT back trajectories for the same site showed that air masses from the Pacific

293   Ocean make it to ROMO (Gebhart et al., 2014), but this is the first chemical evidence of marine

294   air masses at ROMO. Other possible contributing factors for the low correlation between

295     $MeONO_2$ and the other alkyl nitrates may be the relatively higher solubility (faster scavenging by

296   precipitation) and longer lifetime (oxidation and photolysis) of $MeONO_2$ (Russo et al., 2010a).

297

298 **_3.3 Nitrogen Deposition_**

299   Atmospheric nitrogen can be deposited to the surface of the earth by wet and dry

300   deposition. Nitrogen in wet deposition comes from activation of cloud condensation nuclei

301   (CCN) and subsequent scavenging of gases and non-activated aerosols by cloud droplets, rain,

302   and snow. Dry deposition is direct deposition of particles and gases to the surface. Dry

303   deposition is more difficult to quantify than wet deposition because it is difficult to measure

304   directly, and modeled estimates can depend on chemistry and environmental factors including

305   relative humidity, temperature, atmospheric turbulence, boundary layer thickness, and the

306   surface to which deposition occurs (Tarnay et al., 2001).

307

308 _Wet Deposition_

309   Consistent with previous ROMO studies (Beem et al., 2010; Benedict et al., 2013a) wet

310   deposition dominated the total nitrogen deposition budget during FRAPPÉ, contributing 0.79 kg

311   N/ha or 85% to total nitrogen deposition (Figure 7). Ammonium contributed 49%, NO_3^-

312   contributed 34%, and organic nitrogen contributed only 2% to total nitrogen deposition for July

313   17-August 31. While the fraction of organic nitrogen measured in the gas phase was much higher

314   than 2% ($\sum R\text{-}ONO_{2(g)} + PAN_{(g)} = 22\%$) this fraction is likely to be lower in precipitation due to

315   the significantly lower solubility of the different organic nitrogen gases (relative to ammonia and

316   nitric acid), and due to potential for loss in collected samples.

317   The fraction of organic nitrogen (ON) within individual events varied greatly in summer

318   2014, from 0% (ON below detection) to 20%. Although the average wet deposition of ON was

319   less than we have previously observed at this location, the upper bound is consistent with

320   measurements during the 2009 RoMANS study, when the average ON fraction in late summer

321   and early fall was at 20% (Benedict et al., 2013a). Understanding the cause for the differences in

322   the two study years is difficult, because we quantify bulk organic nitrogen and not individual

323   species, which provides little information on source types.

324   At the measurement site in ROMO average precipitation from July to September for the

325   period of 1995-2016 is 179 mm. Annually the changes can be quite large; the standard deviation

326   is 98 mm. Table 2 summarizes the precipitation and wet nitrogen deposition for 2009, 2010, and

327   2014-2016. In 2014 total precipitation from July to September was well above average (222

328   mm) and a large fraction of it (63 mm or 32%) fell during upslope wind events (surface winds

329   70-180°), resulting in high wet deposition values. This is a consistent trend we observed at the

330   ROMO site, years with high precipitation, especially large upslope precipitation fractions tend to

331   have the highest wet N deposition (for example 2009). For the years we have data, 2015 is a case

332   with a lower fraction of precipitation occurring during upslope flow conditions and the lowest

333   wet N deposition likely due to variations in synoptic and local circulation. The variability in

334   precipitation patterns is an important driver in the total N deposition observed due to the

335   importance of wet deposition at the site. Additionally, the fraction of reduced nitrogen or

336   oxidized in the wet deposition do not show any trend with the amount or fraction of precipitation

337   associated with upslope flow, or the fraction of time upslope occurred. Specifically, the largest

338   reduced fraction (66%) was measured in 2016 and the smallest (46%) in 2009 and neither of

339   these years stand out in the parameters we've examined in Table 2.

340

341   *Dry Deposition*

342   For estimating dry deposition during FRAPPÉ, we used a multi-faceted approach,

343   depending on the data. For daily data, we used the monthly average diurnal cycle of deposition

344   velocity (V_d) from CASTNET (U.S. Environmental Protection Agency Clean Air Markets

345   Division, 2016b) to determine V_d for HNO_3, NO_3^-, and NH_4^+, and then applied these hourly V_d

346   values to the 24 hour average concentrations observed (average $V_d(HNO_3)$=1.8 cm/s,

347    $V_d(PM_{2.5})$=0.20 cm/s). The diurnal cycle for V_d was based on monthly average hourly values of

348   all available deposition velocities at the ROMO site (1/1995-1/2014). For NH_3, which is

349   measured at higher time resolution (1-hr), hourly averages were taken from historical data

350   (1/1995-1/2014) for $V_d(HNO_3)$ and were scaled by 0.7 based on a literature survey of co-located

351   HNO_3 and NH_3 V_d measurements (Benedict et al., 2013b,a) (average $V_d(NH_3)$ = 1.25 cm/s).

352   This may overestimate actual net deposition of NH_3 given the importance of bi-directional

353   exchange (Li et al., 2016; Wentworth et al., 2016). Finally, for other gas phase nitrogen species

354   that are not measured or modeled by CASTNET, we examined literature values of fluxes and

355   deposition velocities to estimate their contributions to the nitrogen deposition budget during

356   FRAPPÉ, as discussed below.

357   Estimating dry deposition of NO_y is difficult due to the variability in NO_y composition

358   across study sites and at different times of year. To that end we have estimated the dry

359   deposition of the separate components measured. Hourly deposition velocities for PAN were

360   taken from Turnipseed et al. (2006) for a Loblolly pine forest in North Carolina (daily average

361   0.52 cm/s). However, we note that Wolfe et al. (2009) published hourly values of PAN

362   deposition velocities for a Ponderosa pine forest in the Sierra Nevada mountains that are

363   significantly lower than Turnipseed values (average = 0.17 cm/s). We use the higher Turnipseed

364   values to provide an upper limit for deposition for PAN. This corresponds to a factor of ~2.7

365 difference in the total dry deposition of PAN based on these estimates of V_d. Dry deposition of

366 alkyl nitrates was estimated using the nighttime V_d (0.13 cm/s) from Russo et al. (2010a), one of

367 the few published studies that estimates an alkyl nitrate deposition velocity. The contribution of

368 dry NO deposition to total N deposition has been neglected, as atmospheric chemical reaction is

369 the primary means of removal in the lower atmosphere due to the low solubility and oxidizing

370 capacity of NO (Wesely & Hicks, 2000) and low NO concentrations. In order to provide some

371 estimate of fluxes of the unspeciated components of NO_z, dry deposition was calculated using

372 the average hourly and monthly (1/1995-1/2014) O_3 deposition velocities from CASTNET

373 (Clarke, Edgerton & Martin, 1997; Schwede et al., 2011) scaled by 0.67 (Wesely & Hicks, 2000)

374 (average $V_d(NO_z)$=0.12 cm/s).

375   Estimated dry deposition contributed 0.14 kg N/ha, or 15%, of total deposition in ROMO

376 during the FRAPPÉ period. Dry deposition was dominated by NH_3 (57%; 0.08 kgN/ha)

377 followed by HNO_3 (17%; 0.024 kgN/ha), PAN (13%; 0.018 kgN/ha), and NO_z (7%; 0.01

378 kgN/ha). Of the dry deposited species, NH_3 contributes the most to total deposition (8.6%).

379 Species that are newly measured in this study have small contributions to total nitrogen

380 deposition, including PAN (2 %), NO_z (1%), and alkyl nitrates (0.1%; 0.005 kgN/ha), which are

381 of similar importance to HNO_3 (2.5%), NH_4^+ (0.8%) and NO_3^- (0.1%) dry deposition.

382   Wet nitrogen deposition is directly measured with ~10% uncertainty and should be used

383 as a lower bound of total nitrogen deposition. Estimating the dry component of the nitrogen

384 deposition budget is fairly uncertain but does provide some idea of its potential importance.

385 Limitations of the method to determine dry deposition used here include using average V_d from

386 the site instead of values for the meteorological conditions during the study, using non-site

387 specific values for PAN and NO_y, and not accounting for bi-directional exchange of NH_3 but

388   using the nitric acid V_d ratio should account for some of this interaction. To truly get a handle on

389   the dry deposition component, and the uncertainty in the estimates made here, direct flux

390   measurements need to be made particularly since the dry components are not insignificant to the

391   total estimated nitrogen deposition budget.

392

393

394   *3.4 Sources Impacting ROMO*

395   The VOC measurements at ROMO during FRAPPÉ provide insight into the array of

396   potential sources and source regions that may contribute to excess nitrogen deposition in the

397   park. In an analysis of the VOC data from FRAPPÉ, Benedict et al. (2018) observed the

398   contribution of several sources impacting O_3 at ROMO, with some days showing more oil and

399   gas influence, while others had an increased urban influence.

400   Here we focus on compounds that help separate urban pollutants from those most likely

401   associated with oil and gas production. Tetrachloroethene (C_2Cl_4) has been used extensively as a

402   tracer for urban air (Simpson et al., 2004) because it is used as a dry cleaning solvent and

403   degreasing agent. Ethane is mainly emitted to the atmosphere during the production, processing

404   and transportation of natural gas (Tzompa-Sosa et al., 2017). Table 3 displays the correlation

405   (R^2-values) between the measured RN species and these two VOC tracers. A significant fraction

406   of the observed variability in NO_y, PAN, and the alkyl nitrates (except $MeONO_2$) can be

407   explained by the variability in these tracers. NO_y is more strongly correlated with the urban

408   tracer, C_2Cl_4, while the alkyl nitrates are more strongly correlated with the oil and gas tracer,

409   ethane. PAN is not strongly correlated with either tracer likely because both sources types (oil

410   and gas/urban), long range transport, and photochemical processes contribute to observed

411   concentrations. The strong correlation between alkyl nitrates and ethane is expected, since the

412   parent compounds of the alkyl nitrates (e.g. propane, butane, and pentane) come from similar

413   sources as ethane (Roberts, 1990). No significant increase in the correlation with any of the RN

414   compounds is observed when moving from a single regression to a multi-linear regression using

415   ethane and C_2Cl_4 (not shown).

416   The ratio of i-butane to n-butane has been used extensively to indicate the relative

417   importance of different VOC source types to an air parcel; low values of this ratio can

418   correspond to "wet" oil and gas production or transport (0.37 Marcellus Shale) (Swarthout et al.,

419   2015) and higher values of this ratio indicate rural air masses (0.52 New Hampshire) (Russo et

420   al., 2010b) or "dry" oil and gas production (1.07 Piceance, 0.685 Uintah) (Helmig et al., 2014;

421   Hilliard, 2016). In Figure 8 the tracer and nitrogen-containing compounds are plotted against the

422   i- to n-butane ratio to show how they align with the air masses measured in Denver during

423   FRAPPÉ (0.45) and a regional Denver-Julesburg (DJ) Basin value measured at the BAO tower

424   (0.40) (Swarthout et al., 2013). Individual points are colored by wind direction to provide some

425   information on the transport of the associated air masses and it is important to note, there is a

426   strong relationship between the i- to n-butane ratio with wind direction. For ethane, the highest

427   mixing ratios were observed when the i- to n-butane ratios were near 0.4, consistent with those

428   observed in the DJ Basin. There was significantly more scatter observed for mixing ratios < 2

429   ppb, suggesting mixing of air masses that have been transported over a longer distance. Elevated

430   mixing ratios of PAN and NO_y were associated with i- to n-butane ratios near both Denver and

431   the DJ Basin, while elevated mixing ratios of the alkylnitrates, which are primarily oxidation

432   products of the light alkanes, were observed when i- to n-butane ratios matched those observed

433   within the nearby DJ basin. For NH_3, there was a lot of scatter in i- to n-butane ratios at mixing

434   ratios below 1.5 ppb; however, higher mixing ratios were associated with i- to n-butane ratios

435   similar to those observed within the nearby DJ basin. This likely results due to oil and gas

436   operations being collocated with extensive agricultural operations in this basin.

437   If we extend the analysis from Figure 6 where we observed the influence of long range

438   transport using high concentrations of $CHBr_3$ and ratios of $MeONO_2/EtONO_2$>3 to the reactive

439   nitrogen species we observe that in some cases the reactive nitrogen species are elevated but not

440   significantly (Figure 9). The concentrations of alkylnitrates and NO_y during periods when long

441   range transport was most likely to occur, $CHBr_3$>1 ppbv and higher ratios of $MeONO_2/EtONO_2$,

442   are low and near zero. PAN shows slight elevation during these conditions which is expected

443   due to the greater potential for long range transport at high altitudes and cooler temperatures.

444   However, the majority of high PAN concentrations were not observed under these conditions.

445   Ammonia shows a different pattern with more spread in the concentrations observed at higher

446     $CHBr_3$, some of this variability may be due to local $CHBr_3$ emissions associated with a waste

447   water treatment plant but there are few data available that examine $CHBr_3$ emissions from this

448   type of source (Gschwend, MacFarlane & Newman, 1985; Carpenter et al., 2005). Using this

449   metric is imperfect due to the potential for other sources to contribute to elevated $CHBr_3$, but still

450   the observations with the high ratio of $MeONO_2/EtONO_2$ are more likely to be from long range

451   transport while the other points are more likely to be associated with transport from the Front

452   Range.

453
454   ***4.0 Conclusions***

455   Measurements made at ROMO during the FRAPPÉ study in 2014 provided an

456   opportunity to add measurements of RN that had not been previously made at the site (PAN,

457   alkyl nitrates) and to try to connect observed species and their abundances with specific tracer

458   species to better understand the source regions. In the atmospheric RN budget the relative

459   importance of urban/combustion and rural/agricultural influence is often viewed as the

460   oxidized/reduced nitrogen ratio; however, the rural eastern plains of Colorado are strongly

461   influenced by both agriculture and oil and gas operations, the latter offering significant NO_x

462   emissions (Duncan et al., 2016). So while RN is dominated by oxidized nitrogen in the gas

463   phase, it is not clear that urban air is the dominant contributor of RN deposition to ROMO. In

464   deposition, reduced nitrogen is the major component. The differing importance of reduced

465   (more in precipitation) and oxidized (more in the atmosphere) nitrogen species in the gas and the

466   aqueous phase is a reflection of the different solubilities and abilities to be scavenged based on

467   the properties of the individual species. It also suggests that emissions from many types of

468   sources are important for the observed air mass composition and deposition at ROMO.

469   In this study we observed evidence that emissions from oil and gas operations, urban

470   sources, and long range transport impact ROMO and affect atmospheric reactive nitrogen. The

471   use of VOC tracers confirmed previous measurement (Benedict et al., 2013c) and modeling

472   (Gebhart et al., 2011; Thompson et al., 2015) studies that identified these sources as important in

473   the region. The spatial overlap of agricultural and oil and gas operation sources in eastern

474   Colorado indicate agriculture is also an important source of reactive nitrogen even though we did

475   not use a specific tracer for the source. Other measurements of ammonia and the other RN

476   species, beyond this study, were made during FRAPPÉ. Specifically, there are mobile and

477   aircraft measurements that should be analyzed to determine if more information about specific

478   sources in NE Colorado can be identified. Further analysis of the extensive FRAPPÉ dataset is

479   beyond the scope of the current study. However, it would be beneficial to do a more

480 comprehensive analysis of the FRAPPÉ aircraft data using the ROMO site as a point of reference

481 to better understand the spatial variability of these species.

482   Previous nitrogen deposition budgets constructed for ROMO lacked NO_y and gas phase

483 organic nitrogen compounds as part of the dry deposition budget (Beem et al., 2010; Benedict et

484 al., 2013a). As seen in previous work, the nitrogen deposition budget at ROMO is dominated by

485 wet deposition, specifically NH_4^+ followed by NO_3^-. Our estimates of dry deposition suggest that

486 reduced nitrogen (specifically NH_3) is the largest contributor to the dry deposition budget. This is

487 the first study in ROMO that includes deposition estimates of PAN (1.9% of total N deposition)

488 and alkyl nitrates (0.06% of total N deposition). Although their contributions were relatively

489 small, it is important to examine all components of the nitrogen deposition budget to better

490 understand the role of various sources to nitrogen deposition and better constrain the deposition

491 budget. Providing tighter constraints would require measurements of dry deposition, rather than

492 the inferential estimates as done here. We also lack information on bi-directional fluxes, of NH_3

493 in particular, needed to better understand the deposition budget at ROMO.

494

495 ***Acknowledgements***

496 The assumptions, findings, conclusions, judgments, and views presented herein are those of the

497 authors and should not be interpreted as necessarily representing the National Park Service.

498 Meteorological data were provided by the National Park Service. We would like to recognize

499 the contributions of the FRAPPÉ/Discover-AQ PIs (Gabriele Pfister-NCAR, Frank Flocke-

500 NCAR, Jim Crawford, NASA) for their contributions in organizing and directing the experiment

501 including the flight and measurement planning and field operations.

502

503 References
504
505 Abeleira A., Pollack IB., Sive B., Zhou Y., Fischer EV., Farmer DK. 2017. Source

506   characterization of volatile organic compounds in the Colorado Northern Front Range

507   Metropolitan Area during spring and summer 2015. *Journal of Geophysical Research:*

508   *Atmospheres* 122:2016JD026227. DOI: 10.1002/2016JD026227.

509 Amec Foster Wheeler. 2016. *Appendix 11: Quality Assurance Plan for Procuring, Installing,*

510   *and Operating NCore Air Monitoring Equipment at CASTNET sites.*

511 Baron JS. 2006. Hindcasting nitrogen deposition to determine an ecological critical load.

512   *Ecological Applications* 16:433–439. DOI: 10.1890/1051-0761.

513 Baron JS., Del Grosso S., Ojima DS., Theobald DM., Parton WJ. 2004. Nitrogen emissions

514   along the Colorado Front Range: Response to population growth, land and water use

515   change, and agriculture. In: DeFries RS, Asner GP, Houghton RA eds. *Geophysical*

516   *Monograph Series*. Washington, D. C.: American Geophysical Union, 117–127.

517 Baron J., Ojima D., Holland E., Parton W. 1994. Analysis of Nitrogen Saturation Potential in

518   Rocky-Mountain Tundra and Forest - Implications for Aquatic Systems. *Biogeochemistry*

519   27:61–82.

520 Beem KB., Raja S., Schwandner FM., Taylor C., Lee T., Sullivan AP., Carrico CM., McMeeking

521   GR., Day D., Levin E., Hand J., Kreidenweis SM., Schichtel B., Malm WC., Collett JL.

522   2010. Deposition of reactive nitrogen during the Rocky Mountain Airborne Nitrogen and

523   Sulfur (RoMANS) study. *Environmental Pollution* 158:862–872. DOI:

524   10.1016/j.envpol.2009.09.023.

525 Bell MD., Phelan J., Blett TF., Landers D., Nahlik AM., Van Houtven G., Davis C., Clark CM.,

526   Hewitt J. 2017. A framework to quantify the strength of ecological links between an

527   environmental stressor and final ecosystem services. *Ecosphere* 8:n/a-n/a. DOI:

528   10.1002/ecs2.1806.

529 Benedict KB., Carrico CM., Kreidenweis SM., Schichtel B., Malm WC., Collett JL. 2013a. A

530   seasonal nitrogen deposition budget for Rocky Mountain National Park. *Ecological*

531   *Applications* 23:1156–1169. DOI: 10.1890/12-1624.1.

532 Benedict KB., Chen X., Sullivan AP., Li Y., Day D., Prenni AJ., Levin EJT., Kreidenweis SM.,

533   Malm WC., Schichtel BA., others 2013b. Atmospheric concentrations and deposition of

534   reactive nitrogen in Grand Teton National Park. *Journal of Geophysical Research:*

535   *Atmospheres* 118:11,875–11,887. DOI: 10.1002/2013JD020394.

536 Benedict KB., Day D., Schwandner FM., Kreidenweis SM., Schichtel B., Malm WC., Collett JL.

537   2013c. Observations of atmospheric reactive nitrogen species in Rocky Mountain

538   National Park and across northern Colorado. *Atmospheric Environment* 64:66–76. DOI:

539   10.1016/j.atmosenv.2012.08.066.

540 Benedict KB., Prenni AJ., Carrico CM., Sullivan AP., Schichtel BA., Collett Jr. JL. 2017.

541   Enhanced concentrations of reactive nitrogen species in wildfire smoke. *Atmospheric*

542   *Environment* 148:8–15. DOI: 10.1016/j.atmosenv.2016.10.030.

543 Benedict KB., Zhou Y., Sive BC., Prenni AJ., Gebhart KA., Fischer EV., Evanoski-Cole A.,

544   Sullivan AP., Callahan S., Schichtel BA., Mao H., Zhou Y., Collett Jr. JL. 2018. Volatile

545   Organic Compounds and Ozone in Rocky Mountain National Park during FRAPPÉ.

546   *Atmos. Chem. Phys. Discuss.* 2018:1–42. DOI: 10.5194/acp-2018-375.

547 Bowman WD., Steltzer H. 1998. Positive feedbacks to anthropogenic nitrogen deposition in

548   Rocky Mountain Alpine tundra. *Ambio* 27:514–517.

549   Brown. S., Dibb, J. E., Stark, H., Aldener, M., Vozella M., Whitlow, S., Williams, E. J., Lerner,

550   B. M., Jakoubek, R., Middlebrook, A. M., DeGouw, J. A., Warneke, C., Goldan, P. D.,

551   Kuster, W. C., Angevine, W. M., Sueper, D. T., Quinn, P. K., Bates, T. S., Meagher, J.

552   F., Fehsenfeld, F. C., Ravishankara, A. R. 2004. Nighttime removal of NOx in the

553   summer marine boundary layer. *Geophysical Research Letters* 31. DOI:

554   10.1029/2004GL019412.

555   Brown SS., Ryerson TB., Wollny AG., Brock CA., Peltier R., Sullivan AP., Weber RJ., Dubé

556   WP., Trainer M., Meagher JF., Fehsenfeld FC., Ravishankara AR. 2006. Variability in

557   Nocturnal Nitrogen Oxide Processing and Its Role in Regional Air Quality. *Science*

558   311:67–70. DOI: 10.1126/science.1120120.

559   Brown SS., Stutz J. 2012. Nighttime radical observations and chemistry. *Chemical Society*

560   *Reviews* 41:6405–6447. DOI: 10.1039/C2CS35181A.

561   Burns DA. 2003. Atmospheric nitrogen deposition in the Rocky Mountains of Colorado and

562   southern Wyoming—a review and new analysis of past study results. *Atmospheric*

563   *Environment* 37:921–932. DOI: 10.1016/S1352-2310(02)00993-7.

564   Burns DA. 2004. The effects of atmospheric nitrogen deposition in the Rocky Mountains of

565   Colorado and southern Wyoming, USA—a critical review. *Environmental Pollution*

566   127:257–269. DOI: 10.1016/S0269-7491(03)00264-1.

567   Carpenter LJ., Wevill DJ., O'Doherty S., Spain G., Simmonds PG. 2005. Atmospheric

568   bromoform at Mace Head, Ireland: seasonality and evidence for a peatland source.

569   *Atmos. Chem. Phys.* 5:2927–2934. DOI: 10.5194/acp-5-2927-2005.

570   CDPHE. 2017.Rocky Mountain National Park Initiative | Department of Public Health and

571   Environment. *Available at https://www.colorado.gov/pacific/cdphe/rocky-mountain-*

572   *national-park-initiative* (accessed February 21, 2017).

573   Clarke JF., Edgerton ES., Martin BE. 1997. Dry deposition calculations for the clean air status

574   and trends network. *Atmospheric Environment* 31:3667–3678. DOI: 10.1016/S1352-

575   2310(97)00141-6.

576   Crosley DR. 1996. NO y Blue Ribbon panel. *Journal of Geophysical Research: Atmospheres*

577   101:2049–2052. DOI: 10.1029/95JD02276.

578   Day DA., Dillon MB., Wooldridge PJ., Thornton JA., Rosen RS., Wood EC., Cohen RC. 2003.

579   On alkyl nitrates, O3, and the "missing NOy." *Journal of Geophysical Research:*

580   *Atmospheres* 108:4501. DOI: 10.1029/2003JD003685.

581   Dingle JH., Vu K., Bahreini R., Apel EC., Campos TL., Flocke F., Fried A., Herndon S., Hills

582   AJ., Hornbrook RS., Huey G., Kaser L., Montzka DD., Nowak JB., Reeves M., Richter

583   D., Roscioli JR., Shertz S., Stell M., Tanner D., Tyndall G., Walega J., Weibring P.,

584   Weinheimer A. 2016. Aerosol optical extinction during the Front Range Air Pollution

585   and Photochemistry Éxperiment (FRAPPÉ) 2014 summertime field campaign, Colorado,

586   USA. *Atmospheric Chemistry and Physics* 16:11207–11217. DOI: 10.5194/acp-16-

587   11207-2016.

588   Duncan BN., Lamsal LN., Thompson AM., Yoshida Y., Lu Z., Streets DG., Hurwitz MM.,

589   Pickering KE. 2016. A space-based, high-resolution view of notable changes in urban

590   NOx pollution around the world (2005–2014). *Journal of Geophysical Research:*

591   *Atmospheres* 121:2015JD024121. DOI: 10.1002/2015JD024121.

592   Fenn ME., Baron JS., Allen EB., Rueth HM., Nydick KR., Geiser L., Bowman WD., Sickman

593   JO., Meixner T., Johnson DW., Neitlich P. 2003. Ecological effects of nitrogen

594   deposition in the western United States. *Bioscience* 53:404–420. DOI: 10.1641/0006-

595   3568(2003)053[0404:EEONDI]2.0.CO;2.

596   Fenn ME., Poth MA., Aber JD., Baron JS., Bormann BT., Johnson DW., Lemly AD., McNulty

597   SG., Ryan DE., Stottlemyer R. 1998. Nitrogen excess in North American ecosystems:

598   Predisposing factors, ecosystem responses, and management strategies. *Ecological*

599   *Applications* 8:706–733. DOI: 10.2307/2641261.

600   Flechard CR., Nemitz E., Smith RI., Fowler D., Vermeulen AT., Bleeker A., Erisman JW.,

601   Simpson D., Zhang L., Tang YS., Sutton MA. 2011. Dry deposition of reactive nitrogen

602   to European ecosystems: a comparison of inferential models across the NitroEurope

603   network. *Atmospheric Chemistry and Physics* 11:2703–2728. DOI: 10.5194/acp-11-2703-

604   2011.

605   Galloway JN., Townsend AR., Erisman JW., Bekunda M., Cai Z., Freney JR., Martinelli LA.,

606   Seitzinger SP., Sutton MA. 2008. Transformation of the Nitrogen Cycle: Recent Trends,

607   Questions, and Potential Solutions. *Science* 320:889–892. DOI:

608   10.1126/science.1136674.

609   Gebhart KA., Malm WC., Rodriguez MA., Barna MG., Schichtel BA., Benedict KB., Collett JL.,

610   Carrico CM. 2014. Meteorological and Back Trajectory Modeling for the Rocky

611   Mountain Atmospheric Nitrogen and Sulfur Study II. *Advances in Meteorology* 2014:1–

612   19. DOI: 10.1155/2014/414015.

613   Gebhart KA., Schichtel BA., Malm WC., Barna MG., Rodriguez MA., Collett JL. 2011. Back-

614   trajectory-based source apportionment of airborne sulfur and nitrogen concentrations at

615   Rocky Mountain National Park, Colorado, USA. *Atmospheric Environment* 45:621–633.

616   DOI: 10.1016/j.atmosenv.2010.10.035.

617 Goulding KWT., Bailey NJ., Bradbury NJ., Hargreaves P., Howe M., Murphy DV., Poulton PR.,

618   Willison TW. 1998. Nitrogen deposition and its contribution to nitrogen cycling and

619   associated soil processes. *New Phytologist* 139:49–58. DOI: 10.1046/j.1469-

620   8137.1998.00182.x.

621 Gschwend PM., MacFarlane JK., Newman KA. 1985. Volatile Halogenated Organic Compounds

622   Released to Seawater from Temperate Marine Macroalgae. *Science* 227:1033–1035.

623 Helmig D., Thompson CR., Evans J., Boylan P., Hueber J., Park J-H. 2014. Highly Elevated

624   Atmospheric Levels of Volatile Organic Compounds in the Uintah Basin, Utah.

625   *Environmental Science & Technology* 48:4707–4715. DOI: 10.1021/es405046r.

626 Hilliard NG. 2016. Volatile organic compound and methane emissions from well development

627   operations in the Piceance Basin. Thesis Thesis. Colorado State University. Libraries.

628 Howarth RW. 2004. Human acceleration of the nitrogen cycle: drivers, consequences, and steps

629   toward solutions. *Water Science and Technology* 49:7–13.

630 Kondo Y., Kawakami S., Koike M., Fahey DW., Nakajima H., Zhao Y., Toriyama N., Kanada

631   M., Sachse GW., Gregory GL. 1997. Performance of an aircraft instrument for the

632   measurement of NOy. *Journal of Geophysical Research: Atmospheres* 102:28663–28671.

633   DOI: 10.1029/96JD03819.

634 LeBauer DS., Treseder KK. 2008. Nitrogen Limitation of Net Primary Productivity in Terrestrial

635   Ecosystems Is Globally Distributed. *Ecology* 89:371–379. DOI: 10.1890/06-2057.1.

636   Lehmann CMB., Bowersox VC., Larson SM. 2005. Spatial and temporal trends of precipitation

637   chemistry in the United States, 1985–2002. *Environmental Pollution* 135:347–361. DOI:

638   10.1016/j.envpol.2004.11.016.

639   Li Y. 2016. Characterizing ammonia concentrations and deposition in the United States. Thesis

640   Thesis. Colorado State University. Libraries.

641   Liu X., Duan L., Mo J., Du E., Shen J., Lu X., Zhang Y., Zhou X., He C., Zhang F. 2011.

642   Nitrogen deposition and its ecological impact in China: An overview. *Environmental*

643   *Pollution* 159:2251–2264. DOI: 10.1016/j.envpol.2010.08.002.

644   Malm WC., Collett Jr JL., Barna MG., Beem KB., Carrico CM., Gebhart KA., Hand JL., Levin

645   EJT., Rodriguez MA., Schichtel BA., Schwandner FM. 2009. *RoMANS:Rocky Mountain*

646   *Atmospheric Nitrogen and Sulfur Study Volume 1*.

647   Owen SM., Leaver DS., Bealey WJ., Wilson R., Reis S., Sutton M. 2011. A new database for

648   time-series monitoring data: the NitroEurope approach. *iForest - Biogeosciences and*

649   *Forestry* 4:226. DOI: 10.3832/ifor0595-004.

650   Parrish DD., Buhr MP., Trainer M., Norton RB., Shimshock JP., Fehsenfeld FC., Anlauf KG.,

651   Bottenheim JW., Tang YZ., Wiebe HA., Roberts JM., Tanner RL., Newman L.,

652   Bowersox VC., Olszyna KJ., Bailey EM., Rodgers MO., Wang T., Berresheim H.,

653   Roychowdhury UK., Demerjiani KL. 1993. The total reactive oxidized nitrogen levels

654   and the partitioning between the individual species at six rural sites in eastern North

655   America. *Journal of Geophysical Research: Atmospheres* 98:2927–2939. DOI:

656   10.1029/92JD02384.

657   Prenni AJ., Levin EJT., Benedict KB., Sullivan AP., Schurman MI., Gebhart KA., Day DE.,

658   Carrico CM., Malm WC., Schichtel BA., Collett JL., Kreidenweis SM. 2014. Gas-phase

659   reactive nitrogen near Grand Teton National Park: Impacts of transport, anthropogenic

660   emissions, and biomass burning. *Atmospheric Environment* 89:749–756. DOI:

661   10.1016/j.atmosenv.2014.03.017.

662 Roberts J. 1990. The Atmospheric Chemistry of Organic Nitrates. *Atmospheric Environment*

663   *Part a-General Topics* 24:243–287. DOI: 10.1016/0960-1686(90)90108-Y.

664 Russo RS., Zhou Y., Haase KB., Wingenter OW., Frinak EK., Mao H., Talbot RW., Sive BC.

665   2010a. Temporal variability, sources, and sinks of C1-C5 alkyl nitrates in coastal New

666   England. *Atmos. Chem. Phys.* 10:1865–1883. DOI: 10.5194/acp-10-1865-2010.

667 Russo RS., Zhou Y., White ML., Mao H., Talbot R., Sive BC. 2010b. Multi-year (2004–2008)

668   record of nonmethane hydrocarbons and halocarbons in New England: seasonal

669   variations and regional sources. *Atmos. Chem. Phys.* 10:4909–4929. DOI: 10.5194/acp-

670   10-4909-2010.

671 Schwede D., Zhang L., Vet R., Lear G. 2011. An intercomparison of the deposition models used

672   in the CASTNET and CAPMoN networks. *Atmospheric Environment* 45:1337–1346.

673   DOI: 10.1016/j.atmosenv.2010.11.050.

674 Simpson IJ., Meinardi S., Blake NJ., Rowland FS., Blake DR. 2004. Long-term decrease in the

675   global atmospheric burden of tetrachloroethene (C2Cl4). *Geophysical Research Letters*

676   31:L08108. DOI: 10.1029/2003GL019351.

677 Sive BC., Zhou Y., Troop D., Wang Y., Little WC., Wingenter OW., Russo RS., Varner RK.,

678   Talbot R. 2005. Development of a Cryogen-Free Concentration System for

679   Measurements of Volatile Organic Compounds. *Analytical Chemistry* 77:6989–6998.

680   DOI: 10.1021/ac0506231.

681   Swarthout RF., Russo RS., Zhou Y., Hart AH., Sive BC. 2013. Volatile organic compound

682   distributions during the NACHTT campaign at the Boulder Atmospheric Observatory:

683   Influence of urban and natural gas sources. *Journal of Geophysical Research:*

684   *Atmospheres* 118:10,614-10,637. DOI: 10.1002/jgrd.50722.

685   Swarthout RF., Russo RS., Zhou Y., Miller BM., Mitchell B., Horsman E., Lipsky E., McCabe

686   DC., Baum E., Sive BC. 2015. Impact of Marcellus Shale Natural Gas Development in

687   Southwest Pennsylvania on Volatile Organic Compound Emissions and Regional Air

688   Quality. *Environmental Science & Technology* 49:3175–3184. DOI: 10.1021/es504315f.

689   Tarnay L., Gertler AW., Blank RR., Taylor GE. 2001. Preliminary measurements of summer

690   nitric acid and ammonia concentrations in the Lake Tahoe Basin air-shed: implications

691   for dry deposition of atmospheric nitrogen. *Environmental Pollution* 113:145–153. DOI:

692   10.1016/S0269-7491(00)00168-8.

693   Thompson TM., Rodriguez MA., Barna MG., Gebhart KA., Hand JL., Day DE., Malm WC.,

694   Benedict KB., Collett JL., Schichtel BA. 2015. Rocky Mountain National Park reduced

695   nitrogen source apportionment. *Journal of Geophysical Research: Atmospheres*

696   120:2014JD022675. DOI: 10.1002/2014JD022675.

697   Thornberry T., Carroll MA., Keeler GJ., Sillman S., Bertman SB., Pippin MR., Ostling K.,

698   Grossenbacher JW., Shepson PB., Cooper OR., Moody JL., Stockwell WR. 2001.

699   Observations of reactive oxidized nitrogen and speciation of NO y during the PROPHET

700   summer 1998 intensive. *Journal of Geophysical Research: Atmospheres* 106:24359–

701   24386. DOI: 10.1029/2000JD900760.

702   Turnipseed AA., Huey LG., Nemitz E., Stickel R., Higgs J., Tanner DJ., Slusher DL., Sparks JP.,

703   Flocke F., Guenther A. 2006. Eddy covariance fluxes of peroxyacetyl nitrates (PANs)

704   and NOy to a coniferous forest. *Journal of Geophysical Research: Atmospheres*

705   111:D09304. DOI: 10.1029/2005JD006631.

706   Tzompa-Sosa ZA., Mahieu E., Franco B., Keller CA., Turner AJ., Helmig D., Fried A., Richter

707   D., Weibring P., Walega J., Yacovitch TI., Herndon SC., Blake DR., Hase F., Hannigan

708   JW., Conway S., Strong K., Schneider M., Fischer EV. 2017. Revisiting global fossil fuel

709   and biofuel emissions of ethane. *Journal of Geophysical Research: Atmospheres*

710   122:2016JD025767. DOI: 10.1002/2016JD025767.

711   U.S. Environmental Protection Agency Clean Air Markets Division. 2016a.Clean Air Status and

712   Trends Network (CASTNET). *Available at www.epa.gov/castnet* (accessed April 27,

713   2016).

714   U.S. Environmental Protection Agency Clean Air Markets Division. 2016b.Clean Air Status and

715   Trends Network (CASTNET). *Available at www.epa.gov/castnet* (accessed July 21,

716   2016).

717   US EPA. 2017. *CASTNET Annual Report 2014*.

718   Wentworth GR., Murphy JG., Benedict KB., Bangs EJ., Collett Jr. JL. 2016. The role of dew as a

719   night-time reservoir and morning source for atmospheric ammonia. *Atmos. Chem. Phys.*

720   16:7435–7449. DOI: 10.5194/acp-16-7435-2016.

721   Wesely M., Hicks BB. 2000. A review of the current status of knowledge on dry deposition.

722   *Atmospheric Environment* 34:2261–2282. DOI: 10.1016/S1352-2310(99)00467-7.

723   Williams EJ., Baumann K., Roberts JM., Bertman SB., Norton RB., Fehsenfeld FC., Springston

724   SR., Nunnermacker LJ., Newman L., Olszyna K., Meagher J., Hartsell B., Edgerton E.,

725   Pearson JR., Rodgers MO. 1998. Intercomparison of ground-based NO y measurement

726   techniques. *Journal of Geophysical Research: Atmospheres* 103:22261–22280. DOI:

727   10.1029/98JD00074.

728   Wolfe GM., Thornton JA., Yatavelli RLN., McKay M., Goldstein AH., LaFranchi B., Min K-E.,

729   Cohen RC. 2009. Eddy covariance fluxes of acyl peroxy nitrates (PAN, PPN and MPAN)

730   above a Ponderosa pine forest. *Atmos. Chem. Phys.* 9:615–634. DOI: 10.5194/acp-9-615-

731   2009.

732   Zaragoza J., Callahan S., McDuffie EE., Kirkland J., Brophy P., Durrett L., Farmer DK., Zhou

733   Y., Sive B., Flocke F., Pfister G., Knote C., Tevlin A., Murphy J., Fischer EV. 2017.

734   Observations of acyl peroxy nitrates during the Front Range Air Pollution and

735   Photochemistry Éxperiment (FRAPPÉ). *Journal of Geophysical Research:*

736   *Atmospheres*:2017JD027337. DOI: 10.1002/2017JD027337.

737
738
739

Figure 1

Map of the study region.

Included are the sampling site (star), cities along the northern Front Range of Colorado, oil and gas wells (pink) (COGCC, 2018) , and confined animal feeding operations (purple), scaled by permitted number of animals allowed (CDPHE).
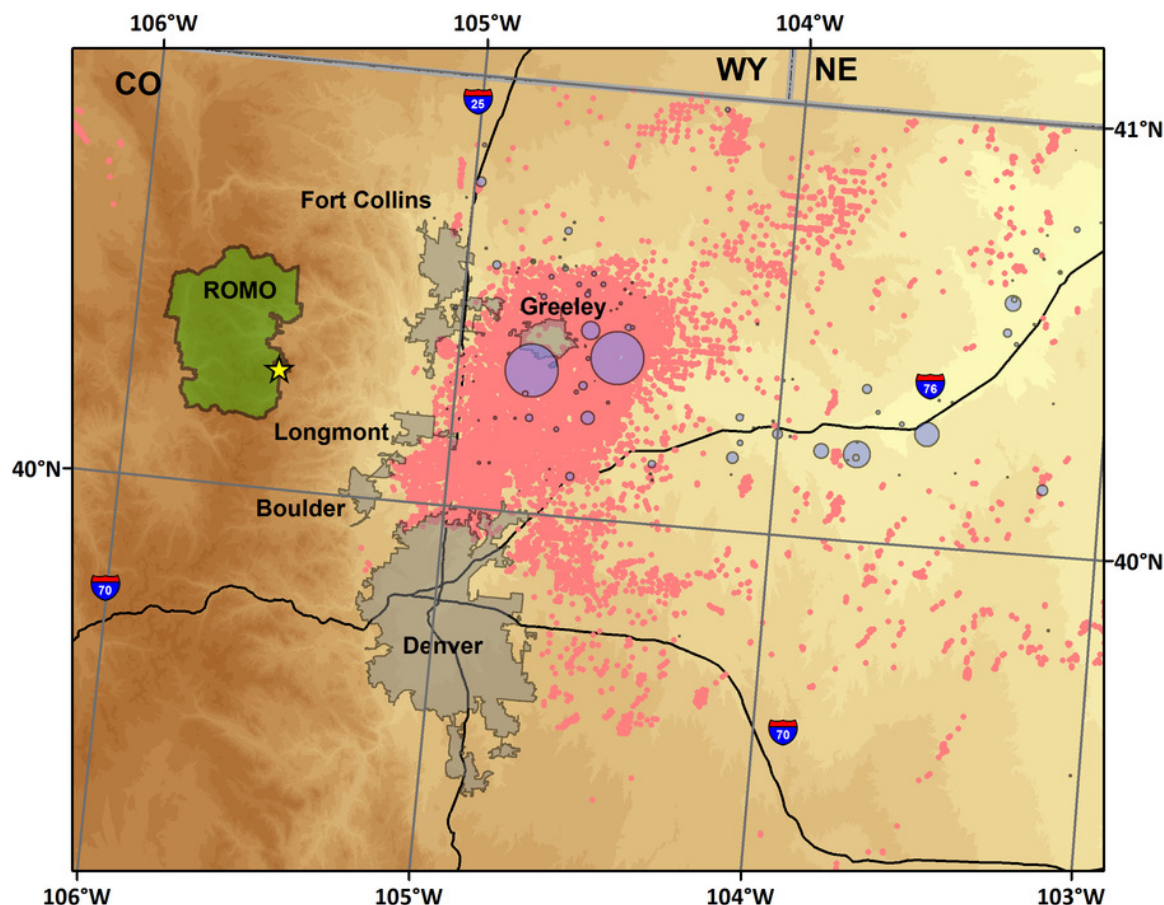
Figure 2

Timelines of reactive nitrogen and tracer species from July 16 to Sept 1, 2014 with wind direction and precipitation.

In (a), the shaded region represents upslope flow at the sampling site.
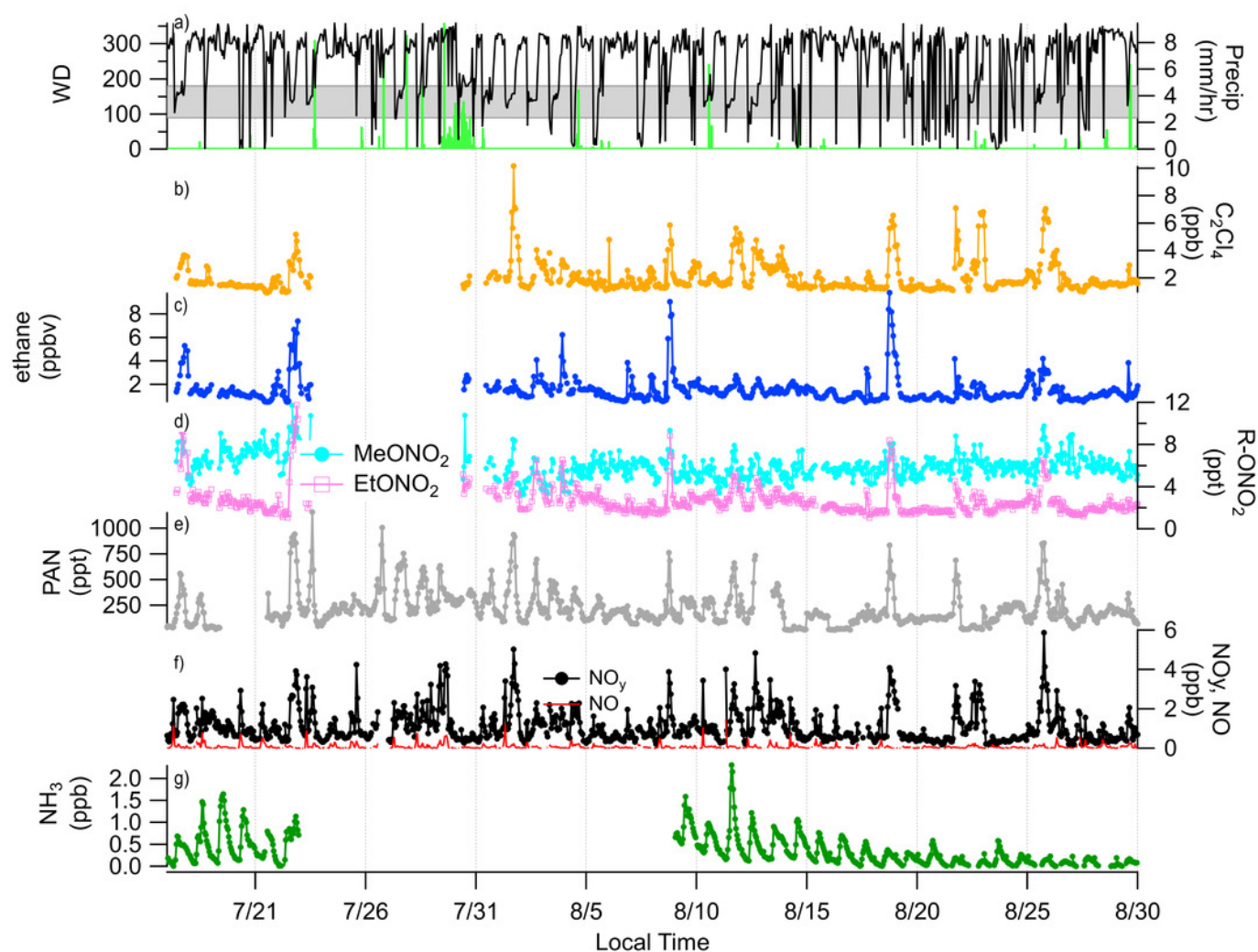
Figure 3

Frequency of PAN concentrations by wind direction.

Distance from the center represents the fraction of time winds were from a given 20° wind sector and the colors in each paddle indicate the relative amounts of time concentrations of PAN were in a given concentration range.
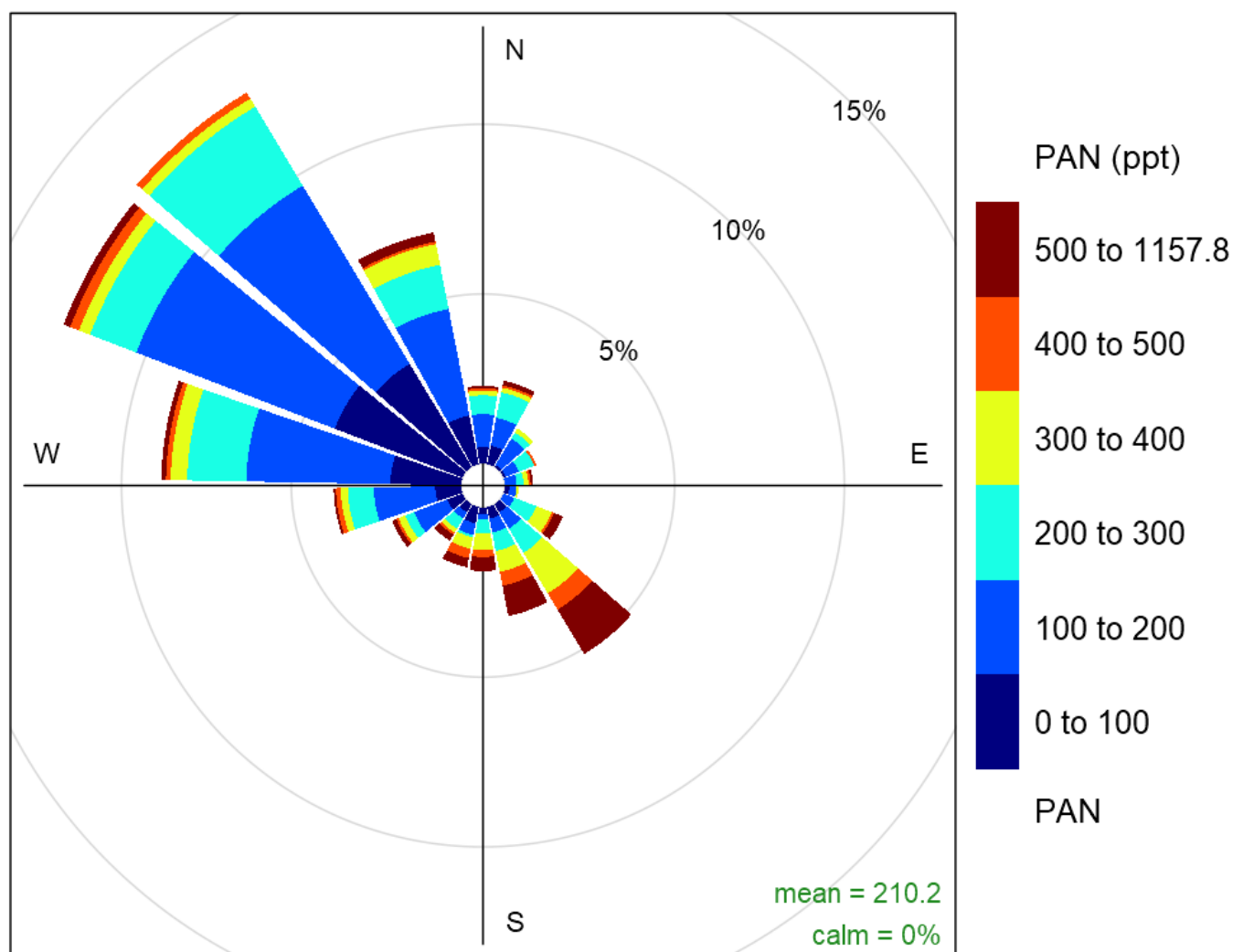
Figure 4

Diurnal averages and standard deviation of key RN and tracer species measured at ROMO from August 9 to August 31 with each valid measurement from every hour shown at the dots.
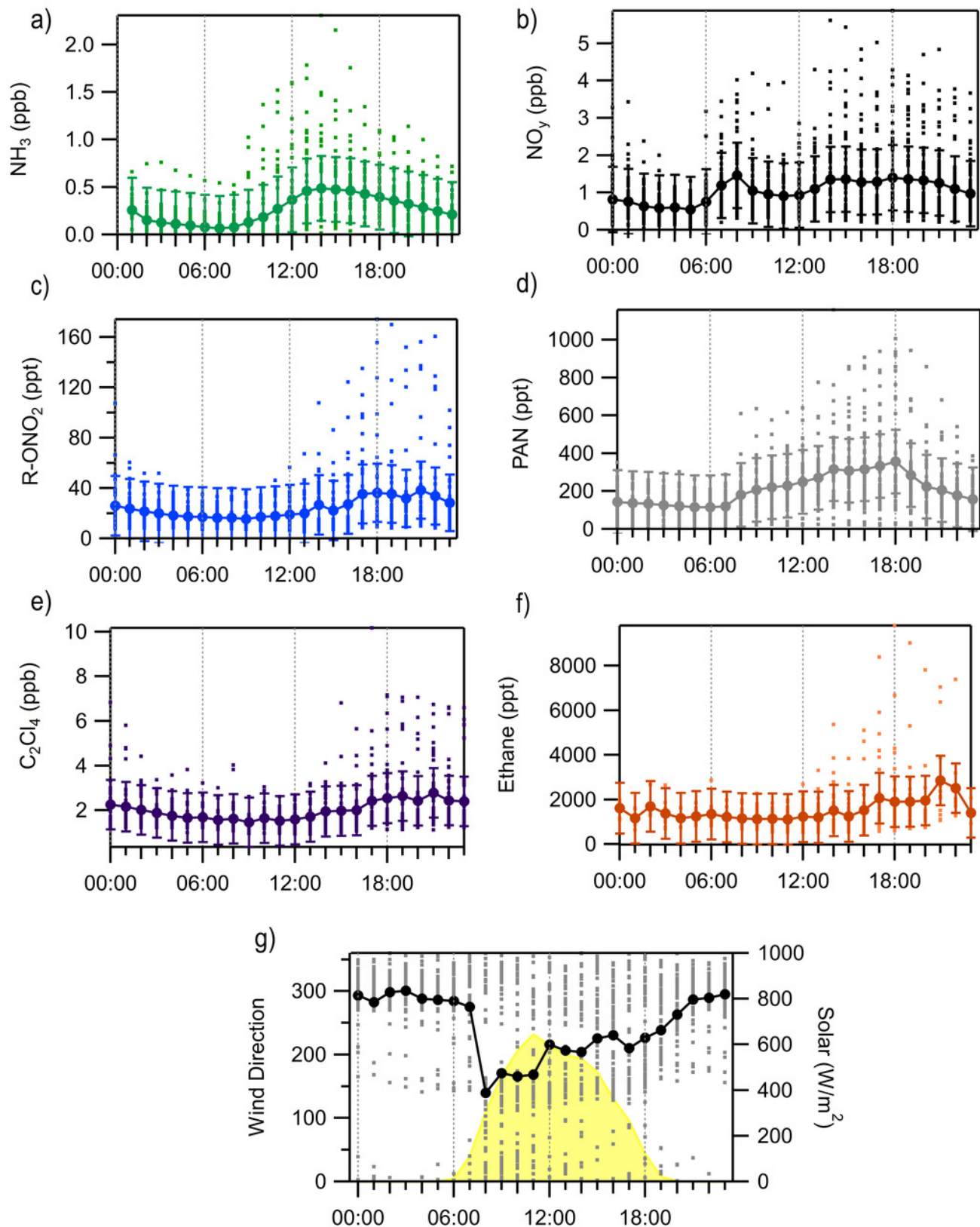
Figure 5

Atmospheric reactive nitrogen budget at ROMO for July 16-August 31 2014.

Concentrations were averaged over the study period and the average total reactive nitrogen concentration was 1.24 ppb. Not included in this assessment are some basic, gas-phase reactive nitrogen species such as amines and acetonitrile.
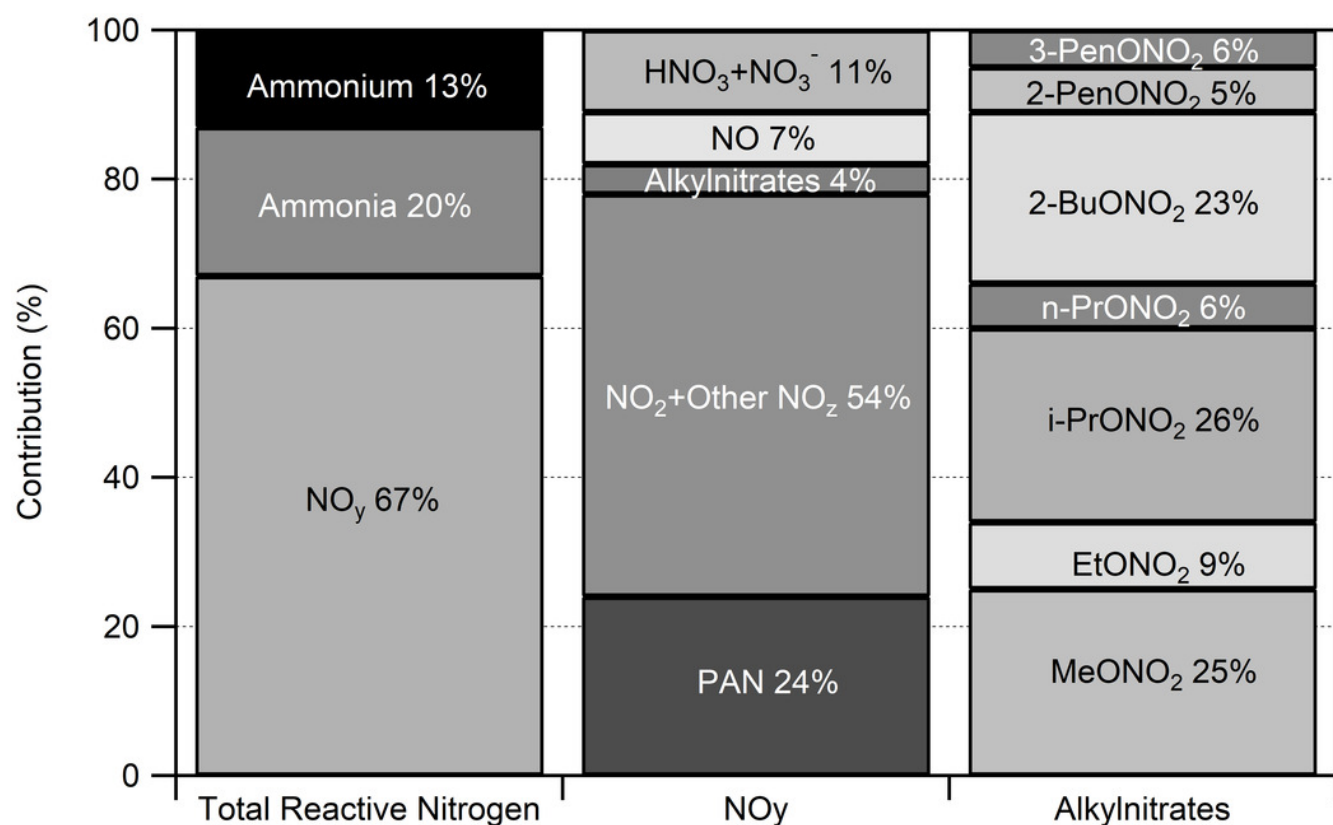
Figure 6

Relationship of methyl nitrate and other alkyl nitrates to ethyl nitrate.

a) i-propyl, n-propyl, and 2-butyl nitrate shown with ethyl nitrate and b) the relationship between methyl and ethyl nitrate colored by mixing ratios of $CHBr_3$ (ppt), a marine air mass tracer highlighting the two sources of methyl nitrate at ROMO.

a)

- ■ i-PrONO$_2$ (r^2= 0.91; slope=4.18)
- + n-PrONO$_2$ (r^2= 0.85; slope=0.95)
- ■ 2-BuONO$_2$ (r^2= 0.85; slope=6.59)

R-ONO$_2$ (ppt)

EtONO$_2$ (ppt)

b)

3:1   2:1   1:1

MeONO$_2$ (ppt)

CHBr$_3$

1.0
0.8
0.6
0.4
0.2

EtONO$_2$ (ppt)
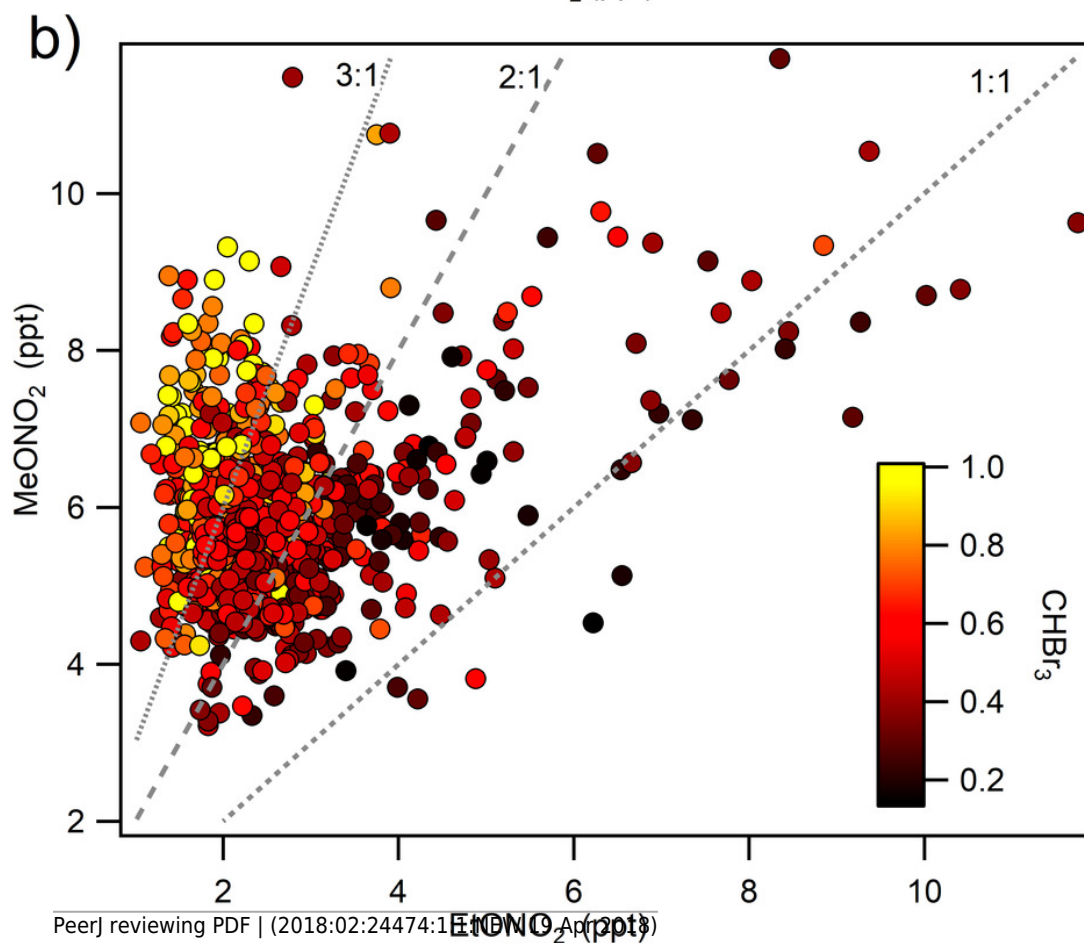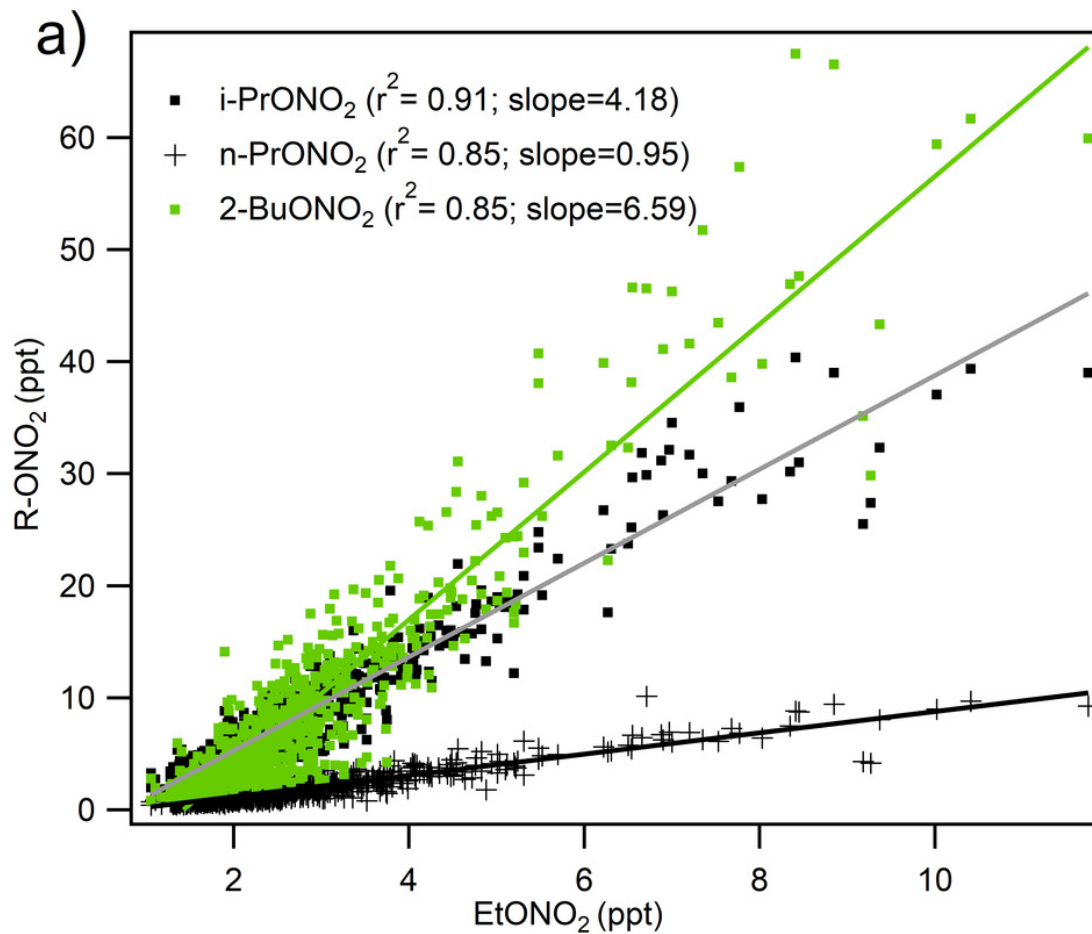
Figure 7

Contributions of the (a) various reactive nitrogen species measured to total nitrogen deposition and (b) breakdown of dry deposition.
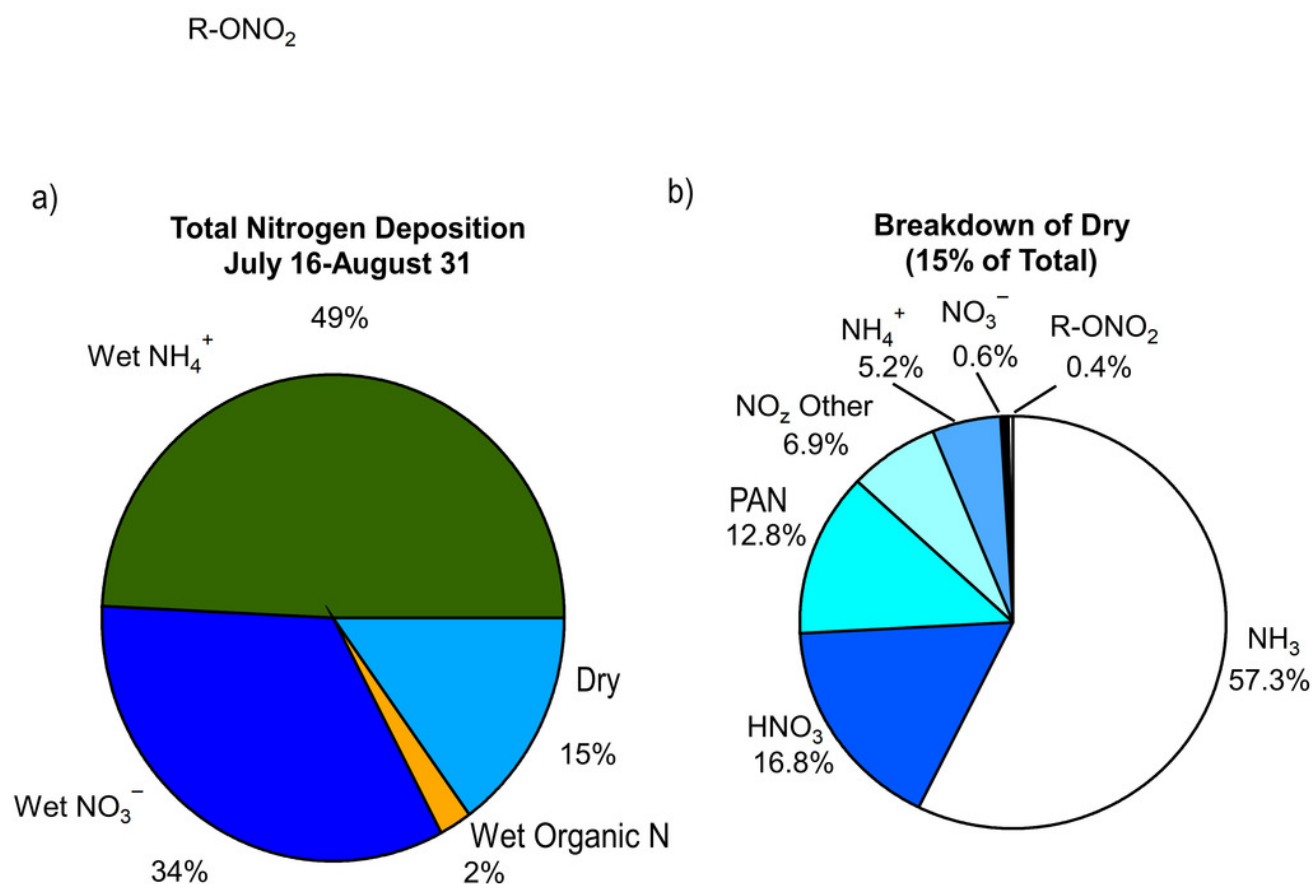
Figure 8

Relationships of the ratio of i-butane to n-butane to various species to separate the influence of Denver (solid) and the agriculture/oil and gas region (dotted) in the Front Range.

The i-butane to n-butane ratio and its relationship to (a) ethane, (b) C_2Cl_4, (c) NH_3, (d) NO_y, (e) alkynitrates, (f) PAN are shown.
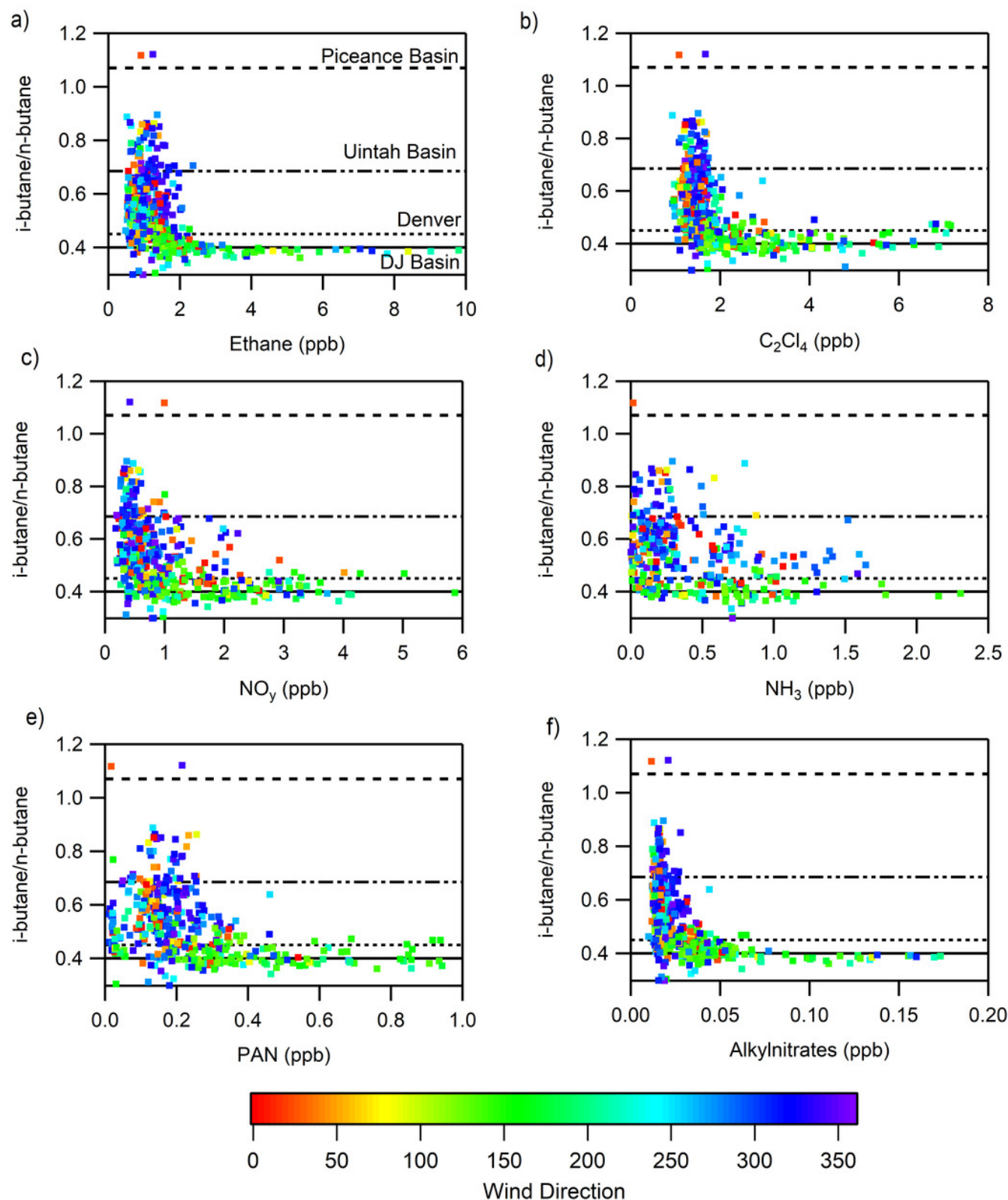
Figure 9

Relationship between reactive nitrogen species and $CHBr_3$ colored by $MeONO_2/EtONO_2$.

All points with a ratio greater than 3 are red.
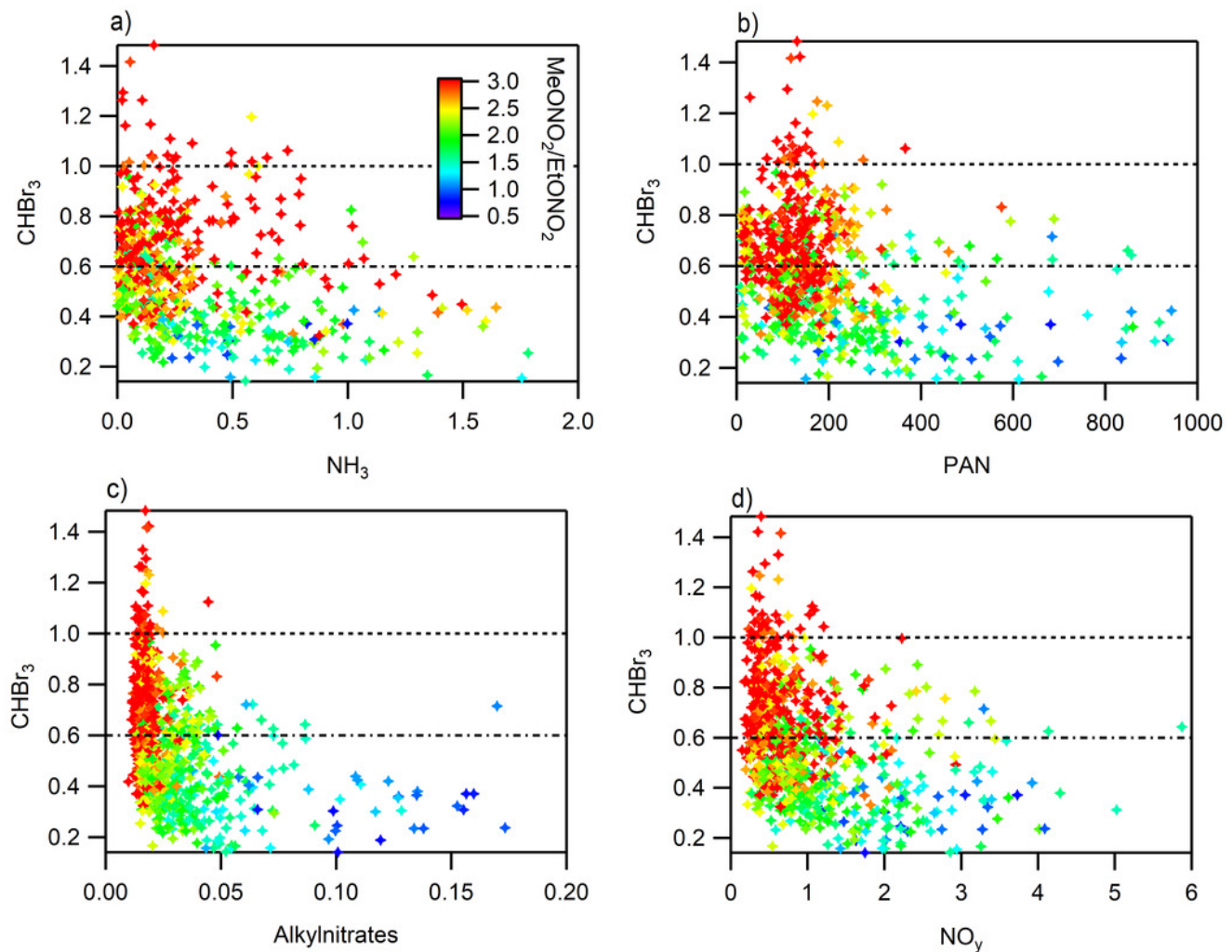
July to August average reactive nitrogen concentrations (ppb).

Also included are the NH_3 and NH_4^+ fraction for the total oxidized and reduced nitrogen for multiple years of measurements made at RMNP. The FRAPPÉ study year is highlighted in bold for ease of comparison.
1   **Table 1. July to August average reactive nitrogen concentrations (ppb) and the NH_3 and**
2   **NH_4^+ fraction for the total oxidized and reduced nitrogen for multiple years of**
3   **measurements made at RMNP. The FRAPPÉ study year is highlighted in bold for ease of**
4   **comparison.**

	NH_3	NH_4^+	HNO_3	NO_3^-	NO_y	NH_4^+ fraction	NH_3 fraction
2009	0.47	0.37	0.10	0.07	1.74	14%	18%
2010	0.38	0.32	0.09	0.05	1.21	17%	20%
2014	**0.34**	**0.20**	**0.06**	**0.03**	**1.05**	**12%**	**21%**
2015	0.43	0.21	0.10	0.04	1.36	11%	22%
2016	0.58	0.25	0.07	0.03	1.22	12%	28%

Summary of precipitation for July-September for the intensive study years in ROMO.

Wet and dry nitrogen deposition are also included for comparison.

1 **Table 2. Summary of precipitation for July-September for the intensive study years in**
2 **ROMO. Wet and dry nitrogen deposition are also included for comparison.**

Year	Precipitation			Fraction of time flow upslope	Wet N Deposition July – Oct (kg N/ha)	[‡]Estimated Dry NH$_3$, HNO$_3$, NH$_4^+$, NO. Deposition (kg N/ha)
	During Upslope (mm)	Total 7/1 - 9/30	Fraction During Upslope			
2009	32.6	102	33%	33%	1.24	0.38
2010[*]	39.9	170.9	26%	23%	0.82	0.25
2014[+]	62.8	221.8	32%	37%	1.37	0.21
2015	17.1	108.1	18%	25%	0.72	0.28
2016	23.3	60.4	30%	27%	0.85	0.35

4 [‡]Dry ammonia deposition was calculated from daily NH$_3$ from denuder measurements to keep the
5 calculation consistent across all study years. [*]July 1- Sept 20, [+]July 7 – Sept 30

Correlation (R^2) between the tracer species (ethane, C_2Cl_4) and the various RN species (ppb).

ᵉ==Manuscript to be reviewed

1 **Table 3. Correlation (R^2) between the tracer species (ethane, C_2Cl_4) and the various RN**
2 **species (ppb).**

	Ethane (R^2)	C_2Cl_4 (R^2)
NH_3	0.01	0.01
NO_y	0.33	0.59
NO	0.003	2E-4
PAN	0.27	0.35
$MeONO_2$	0.05	0.05
$EtONO_2$	0.68	0.42
$i\text{-PrONO}_2$	0.79	0.47
2-BuONO_2	0.85	0.44
2-PenONO_2	0.87	0.42
3-PenONO_2	0.86	0.44